
SPE 93976

# Development of a Thermodynamic Model and Reservoir Simulator for the $CH_4$, $CO_2$, and $CH_4$-$CO_2$ Gas Hydrate System

T. Zhu, UAF; B.P.McGrail, PNNL; A.S.Kulkarni, UAF; M.D.White, PNNL; and H. Phale and D.Ogbe, UAF



This paper was prepared for presentation at the 2005 SPE Western Regional Meeting held in Irvine, CA, U.S.A., 30 March – 1 April 2005.



## Abstract

An equation of state (EOS) software module was developed for $CH_4$, $CO_2$, and $CH_4$-$CO_2$ mixed hydrates by using VanderWall-Platteeuw model. The model is based on classical thermodynamics and is used to predict the thermodynamic behavior of gas hydrates including pressure and temperature at which gas hydrates form. A numerical scheme was developed for solving Lw-V-H and I-V-H equilibrium conditions for bulk hydrate formation from pure water and gas. The model was further extended to determine hydrate equilibrium conditions in the presence of salt. The results calculated from the model were in close agreement with the experimental data reported in literature. One of the contributions of this work is that the proposed model can predict hydrate dissociation pressures at temperatures above 285 K more accurately than any of the existing available modules. The new EOS has been implemented in the multiphase flow simulator STOMP-$CO_2$ developed at PNNL for simulating geological storage of carbon dioxide. Simple reservoir simulations were performed with the new module to examine decomposition of methane hydrate and formation of $CO_2$-hydrate as a new means of natural gas production from gas hydrate reservoirs.

## Introduction

Methane hydrates are clathrate structures that trap methane molecules in a solid ice-like phase, and are formed under conditions of high pressure and low temperature. Conditions for formation of these structures exist on sea bottoms, as well as under permafrost areas. If natural gas can be produced from these structures, total energy reserves are estimated to be far larger than from all conventional fossil fuel reserves combined. Conventional methods of methane recovery from gas hydrate deposit include depressurization, thermal stimulation, inhibitor injection, or a combination of these methods. Depressurization is the most often considered method for commercial production of hydrates (Sloan, 1998). It can effectively dissociate gas hydrate but the endothermic nature of the hydrate decomposition will decrease reservoir temperature, which may temporarily lower production rate. Thermal stimulation provides heat needed to dissociate the hydrate but with some unavoidable heat loss to the host rock. Another method that has been discussed for gas hydrate production involves the injection of $CO_2$.

The idea of swapping $CO_2$ for $CH_4$ in gas hydrates was first advanced by Ohgaki et al. (1996). Their concept involves injecting $CO_2$ gas, which is then allowed to equilibrate with methane hydrate along the three-phase equilibrium boundary. Because of the difference in chemical affinity for $CO_2$ versus methane in the structure I hydrate, the mole fraction of methane would be reduced to approximately 0.48 in the hydrate and rise to a value of 0.7 in the gas phase at equilibrium. However, Ohgaki et al. (1996) didn't address the important issue of the kinetics of the reaction. Recently, McGrail et al. (2004) determined the mass transfer rates of $CO_2$ penetration through methane hydrates. Their work showed that the calculated rates of $CO_2$ penetration into methane hydrates are slow. They further proposed a new concept for enhanced gas hydrate recovery (EGHR). The process involves injection of a $CO_2$-Water microemulsion in hydrate bearing porous media at a temperature higher than the stability point of methane hydrate. It decomposes crystalline methane hydrate lattice and releases the enclathrated gas. Sensible heat of emulsion and heat of formation of the $CO_2$ hydrate provide a low grade heat source for further dissociation of methane hydrates.

A key aspect in the design and interpretation of the proposed method is numerical simulation. The purpose of this work is development of a gas hydrate reservoir model to validate the feasibility of above method on the field scale. It is important to determine the possibility of existence of hydrates for a given pressure temperature conditions in the reservoir. The model discussed here determines the phase equilibrium conditions of hydrate formation. It can predict gas hydrate equilibrium pressure for a temperature. The energy balance will determine pressure and temperature in the reservoir. If the pressure calculated is less than the hydrate equilibrium pressure, it signifies absence of hydrates. On the other hand, if the calculated pressure is greater than the hydrate equilibrium pressure, it indicates existence of hydrates. The numerical

scheme developed in this work can predict I-H-V (Ice-Hydrate-Vapor), $L_w$-H-V (Water-Hydrate-Vapor) equilibrium conditions for $CH_4$, $CO_2$, and $CH_4$-$CO_2$ hydrates. The model is further extended to account for the effect of salinity on gas hydrate phase equilibrium. The presence of salt decreases the activity of water and shifts the gas hydrate phase equilibria towards higher pressures. Pitzer's activity coefficient model is used to calculate reduced activity of water due to salt. The results obtained from the modeling work are compared with the available experimental data and CSMHYD (Hydrate equilibrium software developed at Colorado School of mines).

## Thermodynamic Model

The model used in this work is based on classical statistical thermodynamics proposed by Vander Waal and Platteeuw (1959). It uses adsorption theory to predict hydrate equilibrium conditions. The method for predicting equilibrium is based on the criterion of equality of chemical potential as below,

$$\mu_H = \mu_w \quad (1)$$

Where $\mu_H$: chemical potential of water in the hydrate phase

$\mu_w$: chemical potential of water in the water rich or ice phase

Using $\mu_\beta$, the chemical potential of an unoccupied hydrate lattice, as the reference state, the condition of equilibrium can be rewritten as,

$$\mu_\beta - \mu_w = \mu_\beta - \mu_H \quad (2)$$

$$\Delta\mu_w = \Delta\mu_H \quad (3)$$

**Calculation of $\Delta\mu_w$:** The chemical potential difference as a function of pressure and temperature can be written as,

$$d\left(\frac{\Delta\mu_w}{RT}\right) = -\left(\frac{\Delta h_w}{RT^2}\right)dT + \left(\frac{\Delta V_w}{RT}\right)dP \quad (4)$$

Where $\Delta h_w$ and $\Delta V_w$ are the enthalpy and volume difference between ice or water and the empty hydrate.

Holder, et al. (1980) provided a simple method to determine the effect of temperature, pressure, and composition on $\Delta\mu_w$ as below,

$$\frac{\Delta\mu_w}{RT} = \frac{\Delta\mu^0}{RT_0} - \int_{T_0}^{T}\frac{\Delta h}{RT^2}dT + \int_0^P \frac{\Delta V}{RT}dP - \ln\gamma_w\psi_w \quad (5)$$

The first term on the right accounts for the chemical potential difference between the theoretical empty hydrate and liquid water at its reference state (273.15K, 0 MPa), the second term represents the change in chemical potential difference due to temperature at zero pressure. The third term accounts for the change in chemical potential difference due to pressure, and the last term accounts for the solubility of gas in the pure water or in the presence of a dissolved inhibitor. The activity coefficient $\gamma_w$, accounts for the nonidealities of the solution. The activity coefficient for water, $\gamma_w$, is taken to be equal to 1.0 when only gas and water systems are studied due to generally low solubility of gases in water.

The temperature dependence of the enthalpy difference is given by,

$$\Delta h_w = \Delta h_w{}^0 + \int_{T_0}^{T}\Delta C_{P_w}dT \quad (6)$$

Where $\Delta h_w{}^0$ is an experimentally determined reference enthalpy difference between the empty hydrate lattice and the water phase. $\Delta C_{P_w}$ is the heat capacity difference between the empty hydrate lattice and the water phase. It is also temperature dependent and can be evaluated by the following relationship,

$$\Delta C_{P_w} = \Delta C_{P_w}{}^0 + b(T - T_0) \quad (7)$$

Where $\Delta C_{P_w}{}^0$ an experimentally determined reference heat capacity difference, and b is a constant fitted to experimental data. Two different relationships must be used depending on whether the water phase is in liquid or solid form. Equations (6) and (7) can be used to evaluate the 2nd term in equation (5). $\Delta V$ in equation (5) is constant and it depends on the type of phase present in the system (liquid or solid).

**Calculation of $\Delta\mu_H$:** As per the equilibrium model stated by Vander Waal and Platteeuw (1959), $\Delta\mu_H$ is expressed by following equation,

$$\Delta\mu_H = -RT\sum_i \nu_i \ln(1 - \sum y_{ki}) \quad (8)$$

Here $y_{ki}$ is the fractional occupancy of the cages defined as fraction of the cavity i occupied by the guest molecule k. It follows the Langmuir's isotherm as below,

$$y_{ki} = \frac{C_{ki} f_k}{1 + \sum_j C_{ji} f_j} \quad (9)$$

Where $C_{ki}$ is the Langmuir constant of hydrate former k in cavity type i, which is determined by integrating the gas-water potential function over the volume of the cavity and $f_K$ is the gas phase fugacity of hydrate guest component evaluated by a separate equation of state (EOS). Vander Waal and Platteeuw (1959) suggested the use of Lennard-Jones potential to represent the interaction between enclathrated gas and hydrate lattice water molecules in their original work. However, Lennard-Jones potential is satisfactory only for small spherical molecules. The use of Kihara Potential function is recommended (Sloan, 1998) since it gives better results for larger polyatomic and rod-like molecules. Using classical statistical mechanics, evaluation of the Langmuir constant for spherical molecules is through following equation,

$$C = \frac{1}{kT}\int_0^{2\pi}\int_0^{\pi}\int_0^{R}\exp\left(-\frac{W}{kT}\right)r^2\sin\theta\, dr\, d\theta\, d\phi \quad (10)$$

Where $W=W(r,\theta,\Phi)$ is the total potential energy of interaction between the enclathrated gas molecule and water molecules at positional coordinates $(r,\theta,\Phi)$ which describe the location of gas molecule within a three dimensional cavity.

One of the underlying assumptions of the VanderWaal Platteeuw model was that a hydrate cavity could be described

as a uniform distribution of water molecules smeared over a sphere of radius R. In this case, a smooth cell potential W(r) is independent of angular coordinates. The model assumes that W(r) is a suitable average of W(r,θ,Φ) without carrying out any averaging. Thus Langmuir constant becomes,

$$C = \frac{4\pi}{kT}\int_0^{(R-a)} \exp(-\frac{W(r)}{kT}) r^2 dr \quad (11)$$

The cell potential is obtained as below,

$$W(r) = 2Z\varepsilon\left[\frac{\sigma^{12}}{R^{11}r}\left(\delta^{10} + \frac{a}{R}\delta^{11}\right) - \frac{\sigma^{6}}{R^{5}r}\left(\delta^{4} + \frac{a}{R}\delta^{5}\right)\right] \quad (12)$$

Where,

$$\delta^N = \frac{1}{N}\left[\left(1 - \frac{r}{R} - \frac{a}{R}\right)^{-N} - \left(1 + \frac{r}{R} - \frac{a}{R}\right)^{-N}\right] \quad (13)$$

Where N is equal to 4, 5, 10, and 11. R is the cell or cavity radius, Z is the coordination number of the cavity and r is the distance of the gas molecule from the centre of the cavity. In Equation (12), and (13) a is the core radius of interaction for gas and water molecules, σ is the core-to-core distance between a gas molecule and a water molecule and ε is the depth of the intermolecular well.

John et al. (1985) redefined the smooth cell Langmuir constant by proposing the incorporation of second and third shell of water molecule. However for the purpose of this work, the method for Langmuir-constant determination is same as described above. The Kihara parameter values as given by Sloan (1998) were used for calculation purpose. The R and Z values for each cavity of structure I are given in Table 1. The Kihara potential parameter values for $CH_4$ and $CO_2$ are listed in Table 2.

## Development of Numerical Scheme

Equation (3) can be written in following form,

$$\Delta\mu_w - \Delta\mu_H = 0 \quad (14)$$

Substituting equation (5), (6), (7), (8), and (9) in equation (14), it becomes,

$$f(P) = f(T) + \frac{1}{23}\ln\left(\frac{1}{1 + Cs * f}\right) + \frac{3}{23}\ln\left(\frac{1}{1 + C_l * f}\right) + \frac{\Delta v}{RT}P$$

$$- \ln \psi_w = 0 \quad (15)$$

Note that equation (15) is applicable only for simple hydrates. Where $f$(T) is function of temperature given as below,

$$f(T) = \frac{\Delta\mu^0}{RT_0} - \int_{To}^{T}\frac{\Delta h}{RT^2}dT \quad (16)$$

Equation (15) is a nonlinear function with unknown P for a given temperature T. It can be solved using Newton Rapson Method as below,

$$P_{new} = P_{old} - \frac{f(P)}{f'(P)} \quad (17)$$

$f$'(P) in equation (17) can be determined as ,

$$f'(P) = -\frac{1}{23}\left(\frac{C_S}{1 + C_S f}\right)\left(\frac{df}{dP}\right) - \frac{3}{23}\left(\frac{C_l}{1 + C_l f}\right)\left(\frac{df}{dP}\right) +$$

$$\frac{\Delta V}{RT} + \left(\frac{d\left(\ln\left(1 - X_g\right)\right)}{dP}\right) \quad (18)$$

The solubility of gas in water can be determined using Henry's law described as following,

$$X_g = \frac{f}{H} \quad (19)$$

Where, $f$ is Fugacity of gas at given temperature and pressure, H is Henry's coefficient for dissolution of gas in water at given temperature and pressure.

Henry's coefficient for dissolution of hydrocarbon in the water is primarily a function of temperature only. Thus equation (18) becomes the following form,

$$f'(P) = -\frac{1}{23}\left(\frac{C_S}{1 + C_S f}\right)\left(\frac{df}{dP}\right) - \frac{3}{23}\left(\frac{C_l}{1 + C_l f}\right)\left(\frac{df}{dP}\right) +$$

$$\frac{\Delta V}{RT} + \frac{1}{H - f}\left(\frac{df}{dP}\right) \quad (20)$$

Equation (19) works well for pressures up to 10 MPa. However, at higher pressures, Henry's coefficient is no longer a function of only temperature and it is necessary to incorporate the effect of pressure. The dependency of Henry's coefficient on pressure is described by following equation (Reid and Prausnitz, 1980).

$$\ln H = \ln H^0 + \frac{V_2^{\infty}(P - P_{VP1})}{RT} \quad (21)$$

Where, $H^0$ is Henry's Coefficient calculated as a function of temperature, $V_2^{\infty}$ is Volume of hydrocarbon in water at infinite dilution, and $P_{VP1}$ is Vapor pressure of solvent at temperature T.

A numerical scheme for hydrate formation from mixture of $CO_2$ and $CH_4$ is developed as below,

$$f(P) = f(T) + \frac{1}{23}\ln\left(\frac{1}{1 + C_{s,CO2} f_{CO2} + C_{s,CH4} f_{CH4}}\right) +$$

$$\frac{3}{23}\ln\left(\frac{1}{1 + C_{l,CO2} f_{CO2} + C_{l,CH4} f_{CH4}}\right) + \frac{\Delta V}{RT}P - \ln\left(X_w\right) \quad (22)$$

Equation (22) can be solved for pressure using Newton Raphson method described above. It should be noted that the fugacities of gases in the pure form are different from fugacities in the mixtures (Prausnitz, 1969). Therefore, pure component EOS can not be used for mixtures of $CO_2$ and $CH_4$.

## Hydrate Phase Equilibrium in the presence of Salt

The presence of salt causes a shift in P-T phase equilibrium curve of hydrates towards higher pressures. Englezos and Bishnoi (1988) proposed a new method to calculate hydrate equilibrium conditions in the presence of salt. Their approach involved use of activity of water, $a_w$ in the place of $\gamma_w\psi_w$ in equation (5). Activity of water can be calculated using Pitzer's activity coefficient model (Pitzer and Mayorga, 1973). The necessary equations are described below,

$$\ln a_w = -\frac{18\nu m}{1000}\Phi \qquad (23)$$

In the above equation, Φ can be calculated as following,

$$\Phi = 1 + \left|Z_m Z_X\right| f^{\Phi} + m\left(\frac{2\nu_m \nu_X}{\nu}\right)B^{\Phi}{}_{MX} +$$

$$m^2\left[2(\nu_M \nu_X)^{1.5}\Big/\nu\right]C^{\Phi}{}_{Mx} \qquad (24)$$

Where $f_{\Phi} = -\frac{A^{\Phi} I^{0.5}}{1 + bI^{0.5}}$ (25)

Where, m is molality of electrolyte in solution, ν is stoichiometric number of moles of ions in one mole of salt, $Z_+$, $Z_-$ are charges on each ion in the salt, I is ionic strength of solution, and $A^{\Phi}$ is Debye-Huckel coefficient.
Correlations for $A^{\Phi}$, $B^{\Phi}{}_{MX,}$ and $C^{\Phi}{}_{MX}$ are available in the literature (Pitzer and Moyorga, 1973, and Bradley and Pitzer, 1979).
The above approach works well at low pressures when the solubility of hydrocarbons in the water is low. However at high pressures, the solubility of hydrocarbons can not be neglected. In that case, the activity of water is calculated by an approach proposed by Narsifar and Moshfeghian (2001) as below,

$$\ln a_w = \ln_{aw,el} + \ln a_{w,gas} \qquad (26)$$

Here $a_{w,el}$ is activity of water in the presence of salt as calculated by Pitzer's activity coefficient model and $a_{w,gas}$ is the activity of water in the presence of gas. Activity of water in the presence of gas can be approximated as the mole fraction of water by Lewis-Randoll rule. Thus, $a_{w,gas} \approx \psi_w$.

## Selection of Reference Properties

The prediction of hydrate phase equilibrium is sensitive to the selection of reference properties. Cao Z. et al. (2002) found out that the value of $\Delta\mu_w{}^0$ was much more sensitive to the three phase equilibrium prediction of hydrates. They found that a difference in $\Delta\mu_w{}^0$ of ±10-20 J/mol results in error of 5%-10% in the predicted hydrate equilibrium pressure. They also found that the uncertainties introduced in hydrate equilibrium pressure prediction due to $\Delta h_w{}^0$ are not significant. They used an ab initio potential method to calculate reference properties for hydrate lattice. Those hydrate reference property values are listed in table 3.

## Calculation of Fugacity of Gases

The calculation of fugacity of $CH_4$ in the pure component state was carried out by an EOS state proposed by Setzmann and Wagner (1991). $CO_2$ fugacity calculation was carried out by an EOS state developed by Span Wagner (1996). As stated earlier, pure component EOS can not be used for calculations of component fugacity in the mixtures. Thus an EOS proposed by Duan et al. (1992) was used for $CO_2$-$CH_4$ mixtures.

## Henry's Coefficient Correlations

The Henry's coefficient of methane for the dissolution in water is given by following correlation. (Sloan, 1998)

$$-\ln H = \frac{H^0{}_{KW}}{R} + \frac{H^1{}_{KW}}{RT} + \frac{H^2{}_{KW}}{R}\ln T + \frac{H^3{}_{KW}}{R}T \qquad (27)$$

Similarly for $CO_2$, a correlation proposed by Battistelli et al. (1997) is used. It has following form.

$$K_h(T) = \sum_{i=0}^{4} B(i)T^i \qquad (28)$$

In the presence of salt, the correlation changes and has been modified by Battistelli et al. (1997) for both $CO_2$ and $CH_4$ gases.
The correction is as below,

$$K_{hb}(T, X) = K_h(T) \times 10^{[mK_b(T)]} \qquad (29)$$

Where $K_{hb}$ is the Henry's coefficient in the presence of salt, $k_b$ is the salting-out coefficient and m is salt molality.

## Results and Discussion

**Pure Methane Hydrate:** The numerical model developed above is used to determine I-H-V (Ice-Hydrate-Vapor) and $L_w$-H-V (Water-Hydrate-Vapor) for bulk methane hydrate formation from pure water and methane. The comparison of the results obtained from this study with the available experimental data (Sloan, 1998), and CSMHYD is as shown in Figure 1. As observed in Figure 1, for I-H-V equilibrium, the results from both CSMHYD and our work are in close agreement with experimental ones. An average error of less than 2% is observed through both methods. However for Lw-H-V equilibrium, above 285 K, CSMHYD under predicts the hydrate phase equilibrium, whereas our model produces results which are in close agreement with experimental ones. An average error of less than 5% is obtained through this work. One of the possible reasons for the improved accuracy is the use of more accurate EOS to determine methane gas fugacity. The EOS used in this work can predict fugacities at higher pressures more accurately.

**Pure $CO_2$ Hydrate:** The numerical model developed in this work can be used to predict I-H-V, Lw-H-V, and Lw-H-$L_{CO2}$ equilibrium. Figure 2 shows the comparison of I-H-V and Lw-H-V equilibrium of $CO_2$ hydrates from this work with experimental data and CSMHYD. As seen in Figure 2, the results from both models matched closely with the experimental data. The comparison of Lw-H-$L_{CO2}$ equilibrium is shown in Figure 3. The results for Lw-H-$L_{CO2}$ show a close match between experimental data and this work. However CSMHYD under predicts the Lw-H-$L_{CO2}$ equilibrium for $CO_2$ hydrates. The reason for this discrepancy by CSMHYD can be attributed to the use of EOS in predicting $CO_2$ fugacities in critical region. The EOS used in this work can predict fugacity of $CO_2$ in the critical region accurately. Hence a close match with the experimental data is observed for Lw-H-$L_{CO2}$ equilibrium.

**$CO_2$-$CH_4$ Mixed Hydrates:** The comparison of the results obtained from this work with the available data (Sloan, 1998) and CSMHYD are summarized in table 4. The table shows a close agreement with the experimental data and our work. The results obtained from our work for different $CH_4$ mole fractions are compared with CSMHYD. Figures 4 and 5 show comparisons of results obtained for 20%, and 40% $CH_4$. One of the limitations of the Duan EOS is that it can not predict behavior of $CO_2$-$CH_4$ mixtures in the critical region accurately. Thus the results obtained in the critical region don't match with the experimental data. However, in the critical region the hydrate equilibrium pressures are very high (>10 MPa). The reservoir pressures are not expected to reach that high. Hence the possibility of hydrate formations in critical region is very low.

**Methane hydrate Phase Equilibrium in the Presence of Salt:** As discussed before, the hydrate equilibrium pressure in the presence of salt is higher as compared to bulk hydrates and increases with increase in salt concentration. The results obtained from modeling work shows similar trend. Figure 6 shows the effect on $CH_4$ hydrate equilibrium pressure for 3 wt% NaCl. A close match is observed between experimental data and our work. The comparison between our work and CSMHYD for 5 and 10 wt% NaCl is shown in Figure 7 and 8, respectively. A close look at these figures indicates that for temperatures lower than 285 K, the hydrate equilibrium pressures from both modules are in close agreement. However, above 285 K, hydrate equilibrium pressures obtained from our work are higher as compared to CSMHYD. There is no experimental data available to validate our results. However the trends observed for bulk hydrate calculations indicate the equilibrium pressures to be that high, thus validating the modeling work.

**$CO_2$ Hydrate Phase Equilibrium in the Presence of Salt:** As observed for methane, the hydrate equilibrium pressures for $CO_2$ were also found to be higher than bulk hydrate equilibrium pressures. Figure 9 and 10 show experimental data for $CO_2$ hydrate equilibrium pressure for 3 and 5.552 wt% NaCl and its comparison with our work and CSMHYD respectively. As seen in these figures, a close agreement between experimental and modeling work is obtained in both cases. As discussed above, the solubility of $CO_2$ in water at high pressures is appreciable and hence it can not be neglected. Figure 11 shows modeling results obtained for 10 wt% NaCl and its comparison with CSMHYD. As observed in the figure, both models are in close agreement for $L_w$-H-V equilibrium. However for $L_w$-H-$L_{HC}$, our work predicts higher pressures as compared to CSMHYD. This is quite similar to the trend observed for pure $CO_2$ hydrates. In critical region, $CO_2$ hydrate equilibrium pressures are quite high. The presence of salt leads to shift of $L_w$-H-V equilibrium to $L_w$-H-$L_{HC}$ equilibrium at lower temperatures as compared to bulk hydrates. Hence Lw-H-$L_{HC}$ equilibrium can be expected to be reached at temperature lower than 282 K, which is upper quadruple temperature for bulk $CO_2$ hydrates. The EOS used for $CO_2$ in this work is quite accurate, especially in the critical region. Hence the results obtained in Figure 11 can be validated to be accurate.

## Conclusion

VanderWaal Platteeuw model has been used by most of the researchers for gas hydrate phase equilibrium calculations. In this work, most of the assumptions of the original model were retained. The results obtained from the modeling work are in close agreement with experimental data and other commercial software. At higher temperatures, especially above 285 K, our model can predict gas hydrate equilibrium more accurately than any other existing models. The main reason for this is the use of a highly accurate equation of state to predict gas and liquid phase fugacities. Our calculations demonstrate that gas hydrate equilibrium can be predicted accurately using original VanderWaal Platteeuw model without affecting its original assumptions. This work shows that an optimized set of different properties including Kihara parameters, hydrate reference properties, and accurate EOS can predict gas hydrate phase equilibrium accurately without any modifications.

## Acknowledgments

This work was supported by the Arctic Energy Technology Development Laboratory (AETDL)/U.S. Department of Energy (DOE) under Contract No. DE-FC26-01NT41248. The authors wish to thank the AETDL/DOE for providing financial support for this work.

## Nomenclature

a = core radius of interaction for gas and water molecules ($A^0$)
$a_w$ = activity of water
$a_{w,el}$ = activity of water in the presence of electrolyte
$a_{w,gas}$ = activity of water in the presence of gas
A = constant
$A^\Phi$ = Debye-Huckel coefficient
b = constant
B = constant
$B^\Phi_{MX}$ = constant
$C_{ki}$ = Langmuir constant ($MPa^{-1}$)
$C_l$ = Langmuir constant for large cage $(MPa)^{-1}$
$C_s$ = Langmuir constant for small cage $(MPa)^{-1}$
$C^\Phi_{MX}$ = constant
f = fugacity of gas (MPa)
$f^\Phi$ = polynomial defined by equation (25)
H = Henry's coefficient (MPa)
$H^0_{Kw}$ = constant
$H^1_{Kw}$ = constant
$H^2_{Kw}$ = constant
$H^3_{Kw}$ = constant
I = ionic strength of solution (moles/kg)
k = Boltzmann's constant ($1.3807\times10^{-23}$ J/K)
$k_b$ = salting out coefficient
$K_h(T)$= Henry's coefficient (MPa)
m = molality of solution (mole/kg)
N = constant
P = pressure (MPa)
$P_{VP1}$ = vapor pressure of solvent at temperature T (MPa)
r = distance of the gas molecule from the centre of the cavity ($A^0$)

$(r,\theta,\Phi)$ = spherical coordinates of a gas molecule entrapped within a hydrate cavity
$R$ = radius of cavity ($A^0$)
$R$ = universal gas constant (8.314 J/mol K)
$T$ = temperature (K)
$T_0$ = reference temperature (273.16 K)
$V_2^{\infty}$ = volume of hydrocarbon in water at infinite dilution ($cm^3$)
$W(r)$ = total potential energy of interaction between the enclathrated gas molecule and water molecules (J/mol)
$X_g$ = solubility of gas (mole/mole)
$\psi_w$ = mole fraction of water
$Y_k$ = cage occupancy (fraction)
$Z$ = coordination number
$Z_m$ = positive charge on ion
$Z_X$ = negative charge on ion
$\delta$ = polynomial defined by equation (13)
$\varepsilon$ = depth of the intermolecular well (J)
$\Delta\mu^0$ = chemical potential difference between the theoretical empty hydrate and liquid water at reference state (273.15K, 0 kPa) (J/mol)
$\Delta\mu_H$ = chemical potential difference between the empty hydrate lattice and the hydrate phase. (J/mol)
$\Delta\mu_w$ = chemical potential difference between the empty hydrate lattice and the water phase. (J/mol)
$\sigma$ = core-to-core distance between a gas molecule and a water molecule ($A^0$)
$\Delta h_w$ = enthalpy difference between ice or water and the empty hydrate. (J/mol K)
$\Delta h_w^0$ = enthalpy difference between the empty hydrate lattice and the water phase at reference state (273.15K, 0 kPa) (J/mol)
$\Delta V_w$ = volume difference between ice or water and the empty hydrate (cc/mol)
$\gamma_w$ = activity coefficient of water
$\gamma_m$ = stoichiometric coefficient for positive ion
$\gamma_X$ = stoichiometric coefficient for negative ion
$\mu_H$ = chemical Potential of water in the hydrate phase (J/mol)
$\mu_w$ = chemical Potential of water in the water rich or ice phase (J/mol)
$\sigma_w$ = core-to-core Kihara Distances for the gas molecules ($A^0$)
$\Delta C_{P_w}$ = heat capacity difference between the empty hydrate lattice and the water phase (J/mol K)
$\Delta C_{P_w}^{\ 0}$ = reference heat capacity difference (J/mol)

## Reference


1. Sloan E.D., JR.: 1998. *Clathrate Hydrates of Natural Gases*, 2nd Edit., Marcel Dekker, Inc. New York.
2. Ohgaki, K., K. Takano, H. Sangawa, T. Matsubara, and S. Nakano.: "Methane Exploitation by Carbon Dioxide from Gas Hydrates - Phase Equilibria for $CO_2$-$CH_4$ Mixed Hydrate System." *J.Chem.Eng. Japan*, 1996, **29(3),** 478-483.
3. Mcgrail, B.P., Zhu, T., Hunter, R.B., White, M.D., Patil, S.L, and Kulkarni, A.S.: "A New Method for Enhanced Production of Gas Hydrates with $CO_2$", in proceedings of the AAPG Hedberg Conference held in Vancouver, Canada, Sept. 12-16, 2004.
4. Vander Waals, J.H. and Platteeuw, J.C.: "Clathrate Solutions", *Adv. In Chem.Phys.*, 1959, **2**, 1-57.
5. Holder G.D. and Corbin G., Papadopoupoulos K.D.: "Thermodynamic and Molecular Properties of Gas Hydrates from Mixtures Containing Methane, Argon and Krypton", Industrial and Engineering Chemistry Fundamental, 1980, **19**,282-286.
6. John, V.T., Papadopoulos, K.D. and Holder, G.D.: "A Generalized Model for Predicting Equilibrium Conditions", *AIChE Journal*, 1985, **31(2)**, 252-259
7. Reid, R.C., J.M. Prausnitz, and B.E. Poling: *The Properties of Gases and Liquids*, McGraw-Hill, New York, New York., 1987, pp: 332-337.
8. Prausnitz, J.M.: *Molecular thermodynamics of fluid phase equilibria*, Prentice Hall Inc., New Jersey, 1969, pp: 89-92.
9. Englezos, P. and Bishnoi, P.R.: "Prediction of gas hydrate formation conditions in aqueous electrolye", *American Institute of Chemical Engineers*, 1988, **34(10)**, 1718-1721.
10. Pitzer K.S. and Mayorga G.: "Thermodynamics of Electrolytes. II. Activity and Osmotic Coefficient for Strong Electrolytes with One or both Ions Univalent.", *The Journal of Physical Chemistry*, 1973, **77(19)**, 2300-2308.
11. Bradley D.J. and Pitzer K.S.: "Thermodynamics of Electrolytes. 12. Dielectric Properties of Water and Debye-Huckel Parameters to $350^0$C and 1 kbar", *The Jouranl of Physical Chemistry*, 1979, **83(12)**, 1599-1603.
12. Nasrifar K. and Mohfeghian M.: "A model for prediction of gas hydrate formation conditions in aqueous solutions containing electrolytes and/or alcohol", *J.Chem.Thermodynamics*, 2001, **33**, 999-1014.
13. Zhitao C., Jefferson W. Tester, and Bernhardt L. Trout: "Sensitivity Analysis of Thermodynamic Reference Properties Using Experimental Data and ab Initio Methods", *J.Phys. Chem. B*, 2002, **106**, 7681-7687.
14. Setzmann, U., and W. Wagner.: "A New Equation of State for Methane Covering the range from the Melting Line to 625 K at Pressures up to 1000 MPa." *J. Phys. Chem. Ref. Data*, 1991, **20(6)**, 1061-1155.
15. Span, R., and W. Wagner.: "A New Equation of State for Carbon Dioxide Covering the Fluid Region from the Triple-Point to 1100 K at Pressures up to 800 MPa.", *J. Phys. Chem. Ref. Data*, 1996, **25(6)**, 1509-1588.
16. Duan, Z., Moller, N., and Weare, J.H.: "An equation of state for the methane-carbon dioxide-water system: II. Mixtures from 50 to 1000 C and 0 to 1000 bar", *Geochimica et cosmochimica acta*, 1992, **56(7)**, 2619-31.
17. Battistelli, A., C. Claudio, and K. Pruess.: "The simulator TOUGH2/EWASG for modelling geothermal reservoirs with brines and noncondensible gas." *Geothermics*, 1997, **26(4)**, 437-464.


**Table 1: Geometry of Structure I Gas Hydrates**

| Structure I | R ($A^0$) | Z |
|---|---|---|
| Small Cavity | 3.95 | 20 |
| Large Cavity | 4.33 | 24 |

**Table 2: Kihara Parameters for $CH_4$ and $CO_2$**

| | $\varepsilon$/K (K) | $\sigma$ ($A^0$) | a ($A^0$) |
|---|---|---|---|
| $CH_4$ | 154.54 | 3.165 | 0.3834 |
| $CO_2$ | 168.77 | 2.9818 | 0.6805 |

**Table 3: Hydrate Reference Properties for Structure I**

| | | |
|---|---|---|
| $\Delta\mu_w^0$ (J/mol) | T=273.16 K | 1236 |
| $\Delta h_w^0$ (J/mol) | T < 273.16 K | 1706 |
| | T > 273.16 K | -4303.5 |
| $\Delta V_w$ (cc/mol) | T < 273.16 K | 3.0 |
| | T > 273.16 K | 4.598 |
| $\Delta C_{Pw}$ (J/mol K) | T < 273.16 K | $0.565 + 0.002(T-T_0)$ |
| | T > 273.16 K | $-38.12 + 0.141(T-T_0)$ |

**Table 4: $CO_2$-$CH_4$ Mixed Hydrate Modeling Results**

| T (K) | % CH4 | Pexpt (MPa) | UAF HYD Module |
|---|---|---|---|
| 273.7 | 90 | 2.52 | 2.4859 |
| 273.7 | 21 | 1.45 | 1.5382 |
| 273.8 | 75 | 2.12 | 2.1628 |
| 274.6 | 86 | 2.59 | 2.5856 |
| 275.8 | 91 | 3.1 | 3.054 |
| 276.4 | 30 | 2.08 | 2.1269 |
| 276.9 | 87 | 3.24 | 3.2436 |
| 277.8 | 92 | 3.83 | 3.7307 |
| 277.8 | 24 | 2.37 | 2.4156 |
| 278.4 | 91.5 | 3.95 | 3.9287 |
| 278.5 | 53 | 2.98 | 2.9645 |
| 278.9 | 70 | 3.46 | 3.4213 |
| 279.1 | 87 | 4.18 | 4.0098 |
| 279.4 | 78 | 3.96 | 3.8157 |
| 279.6 | 29 | 3 | 3.011 |
| 279.6 | 25 | 2.97 | 2.9709 |
| 280.2 | 32 | 3.28 | 3.2588 |
| 280.9 | 68 | 4.24 | 4.1508 |

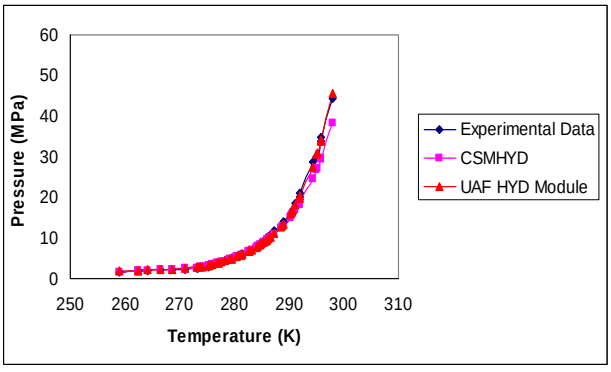


**Figure 1: Methane Hydrate Phase Equilibrium**

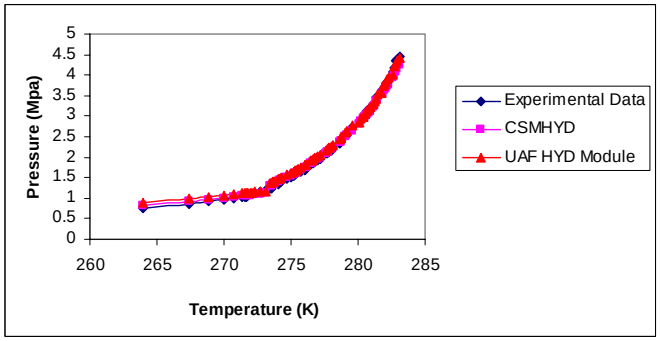


**Figure 2: $CO_2$ Hydrate Phase Equilibrium (I-H-V and Lw-H-V Equilibrium)**

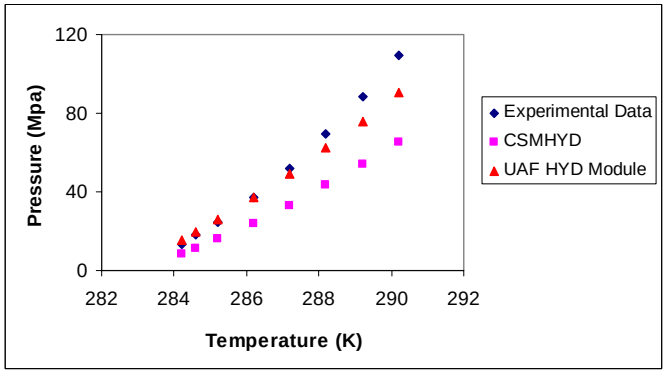


**Figure 3: $CO_2$ Hydrate Phase Equilibrium (Lw-H-$L_{CO2}$ Equilibrium)**

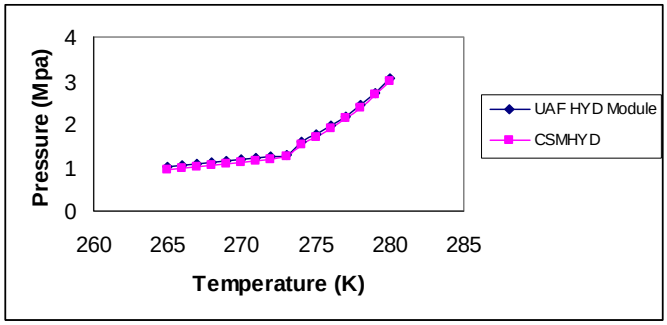


**Figure 4: $CO_2$-$CH_4$ Mixed Hydrate Phase Equilibrium (20% $CH_4$)**

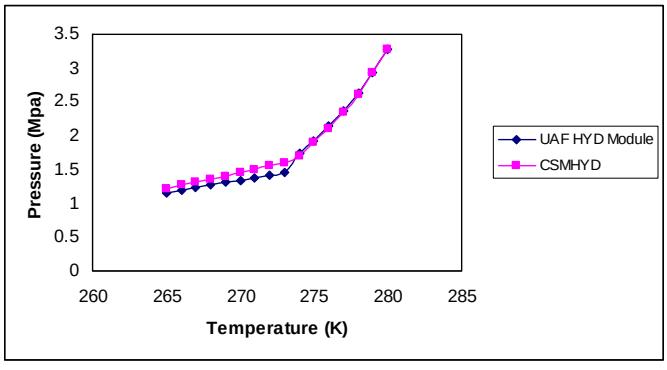


**Figure 5: $CO_2$-$CH_4$ Mixed Hydrate Phase Equilibrium (40% $CH_4$)**

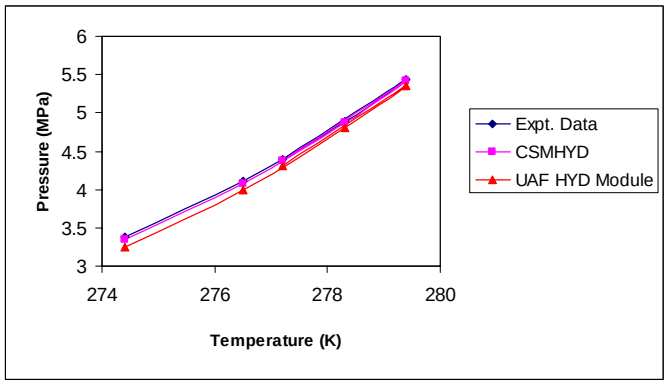


**Figure 6: $CH_4$ Hydrate Equilibrium Conditions in the presence of Salt (NaCl=3%)**

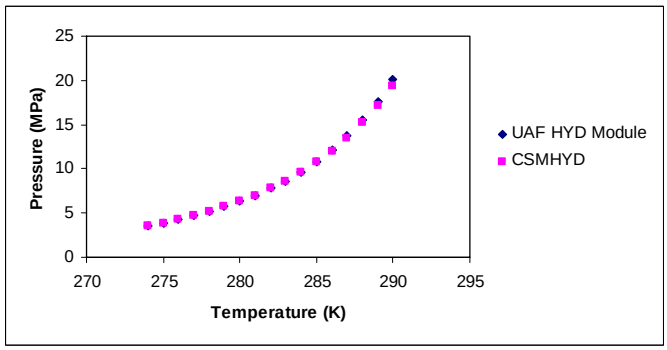


**Figure 7: $CH_4$ Hydrate Equilibrium Conditions in the presence of Salt (NaCl=5%)**

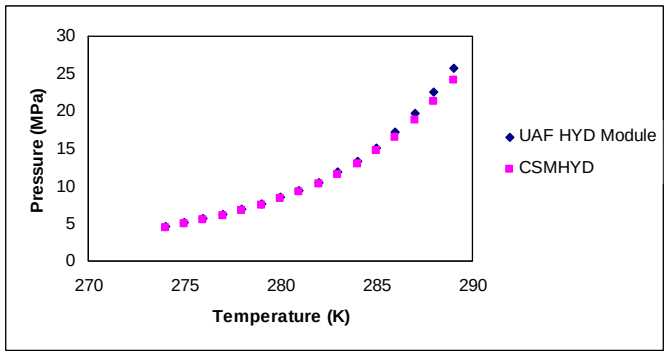


**Figure 8: $CH_4$ Hydrate Equilibrium Conditions in the presence of Salt (NaCl=10%)**

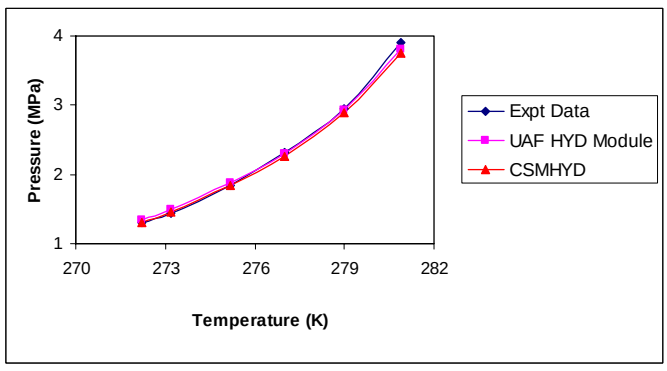


**Figure 9: $CO_2$ Hydrate Phase Equilibrium in the presence of Salt (NaCl=3%)**

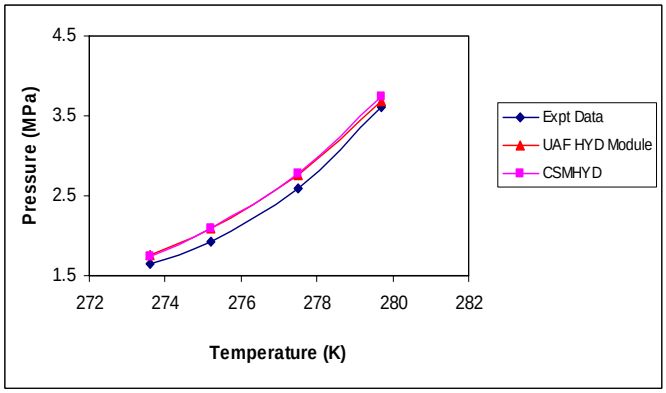


**Figure 10: $CO_2$ Hydrate Phase Equilibrium in the presence of Salt (NaCl=5.552%)**

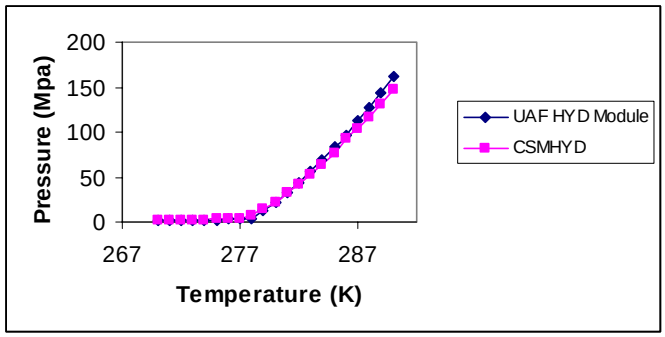


**Figure 11: $CO_2$ Hydrate Phase Equilibrium in the presence of Salt (NaCl=10%)**